# Integrated omics-based analysis reveals distinct microbial-metabolite interaction networks in eosinophilic and non-eosinophilic chronic rhinosinusitis with nasal polyps in a Chinese population

Hailing Zhang[1,#], Xiaoxue Zi[1,#], Xu Li[2], Tingting Gao[2], Hongping Zhang[1], Hongyang Zhang[1], Xu Liang[1], Lili Zhi[2,*], Peng Jin[1,*]

**Rhinology 64: 2,** 0 - 0, 2026
https://doi.org/10.4193/Rhin25.166

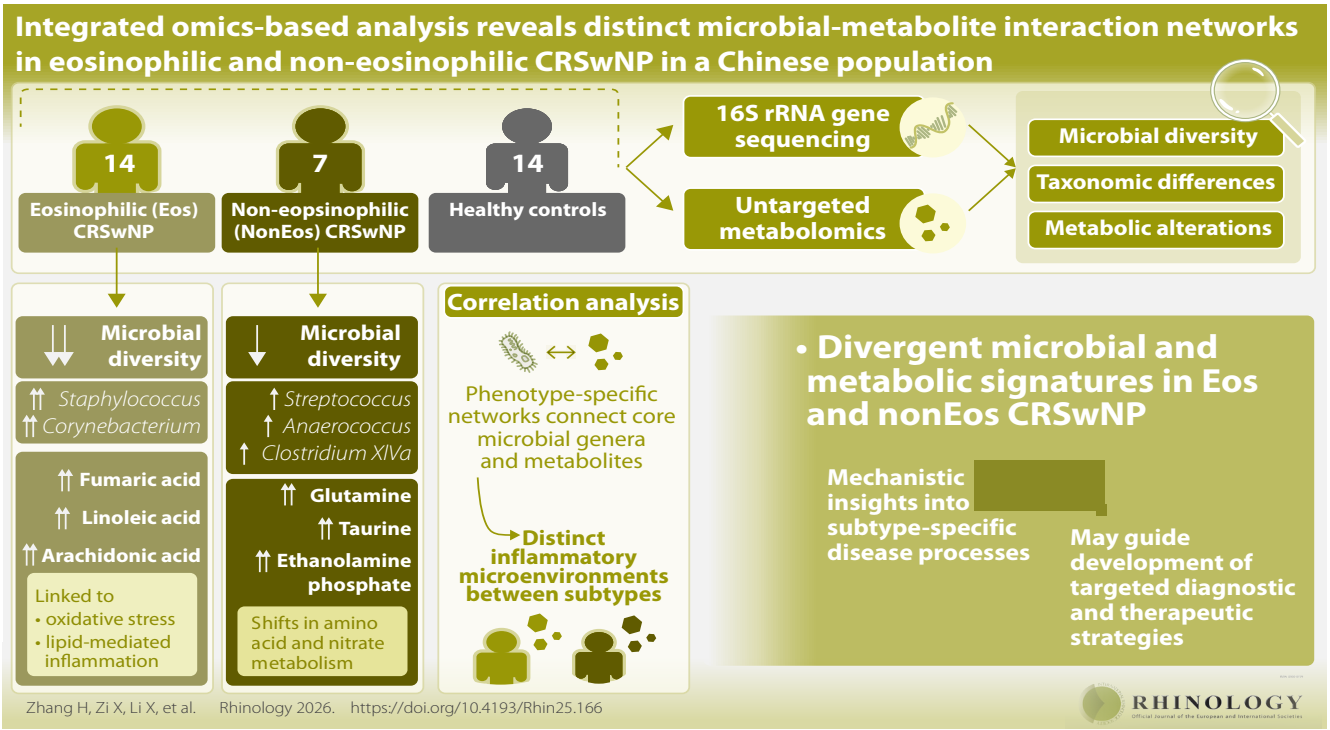


## Abstract

**Background**: Chronic rhinosinusitis with nasal polyps (CRSwNP) is a heterogeneous inflammatory condition often classified into eosinophilic (Eos) and non-eosinophilic (nonEos) subtypes. While microbial dysbiosis and metabolic disturbance are known contributors to CRSwNP, the interplay between sinonasal microbiota and local metabolic activity remains unclear. **Methods**: We conducted 16S rRNA gene sequencing and untargeted metabolomics on sinonasal swabs and tissue samples from patients with Eos-CRSwNP (n = 14), nonEos-CRSwNP (n = 7), and healthy controls (n = 14). Microbial diversity, taxonomic differences, and metabolic alterations were analyzed. Spearman correlation and network modeling were used to explore phenotype-specific microbiota–metabolite interactions and pathway enrichment. **Results**: Eos-CRSwNP was characterized by reduced microbial diversity and increased abundance of *Staphylococcus* and *Corynebacterium*, along with elevated levels of fumaric acid, linoleic acid, and arachidonic acid—metabolites linked to oxidative stress and lipid-mediated inflammation. In contrast, nonEos-CRSwNP exhibited greater microbial richness, with enrichment of *Streptococcus*, *Anaerococcus*, and *Clostridium XlVa*, and metabolic shifts in amino acid and nitrogen metabolism, including increased glutamine, taurine, and ethanolamine phosphate. Correlation analysis revealed phenotype-specific networks connecting core microbial genera and metabolites, suggesting distinct inflammatory microenvironments between subtypes. **Conclusion**: Our integrated multi-omics analysis highlights divergent microbial and metabolic signatures in Eos and nonEos CRSwNP. These findings offer mechanistic insights into subtype-specific disease processes and may guide the future development of targeted diagnostic and therapeutic strategies.

**Key words**: chronic rhinosinusitis, nasal polyps, microbiome, metabolomics, eosinophilic, non-eosinophilic, omics integration

## Introduction

Chronic rhinosinusitis with nasal polyps (CRSwNP) is a persistent inflammatory disorder of the sinonasal mucosa that significantly impacts patients' quality of life through symptoms such as nasal obstruction, facial pressure, loss of smell, and rhinorrhea [1, 2]. Histologically, CRSwNP is defined by mucosal inflammation and the formation of benign polypoid growths, often requiring repeated surgical and medical interventions. Increasing evidence supports the concept that CRSwNP is not a single disease entity but a heterogeneous syndrome encompassing multiple phenotypes with distinct immunopathological mechanisms [3-6]. Among these, eosinophilic CRSwNP (Eos-CRSwNP) and non-eosinophilic CRSwNP (nonEos-CRSwNP) represent two major inflammatory subtypes, particularly relevant in clinical management and therapeutic response. Eos-CRSwNP is strongly associated with Type 2 helper T cell (Th2)-mediated inflammation, characterized by elevated interleukin (IL)-4, IL-5, and IL-13 levels, and marked eosinophilic infiltration in the nasal mucosa [7-9]. This subtype is frequently comorbid with asthma, allergic rhinitis, and aspirin-exacerbated respiratory disease (AERD), and typically responds well to corticosteroids and emerging biologic therapies targeting IL-5 or IL-4Rα [10-12]. In contrast, nonEos-CRSwNP is more heterogeneous, often associated with neutrophilic inflammation and mixed Th1/Th17 immune responses. This phenotype is more commonly observed in Asian populations and tends to be more resistant to corticosteroids and conventional anti-inflammatory treatments [13,14]. Despite these broad distinctions, the mechanisms underlying phenotypic divergence remain only partially understood, and current diagnostic approaches rely heavily on histopathology rather than functional profiling.

Recent studies have highlighted the potential role of the nasal and sinonasal microbiome in modulating mucosal inflammation in CRSwNP [15-17]. The nasal cavity is colonized by a diverse community of commensal and opportunistic microbes that may influence epithelial barrier function, immune activation, and tissue remodeling [18,19]. Dysbiosis—defined as an imbalance in the microbial community—has been observed in CRSwNP, with alterations in the relative abundance of key genera such as *Staphylococcus*, *Corynebacterium*, and *Streptococcus* [20,21]. However, microbial composition alone provides limited insight into disease mechanisms. The metabolites produced or influenced by the microbiota may act as bioactive mediators that link microbial activity to host inflammation.

Metabolomics, the comprehensive profiling of small-molecule metabolites in biological systems, offers a powerful lens for investigating local biochemical activity within inflamed sinonasal tissues. Inflammatory conditions are frequently associated with metabolic reprogramming, and in CRSwNP, emerging evidence suggests alterations in lipid metabolism, oxidative stress pathways, and amino acid biosynthesis [22-24]. Microbial-derived metabolites, such as short-chain fatty acids, polyamines, and eicosanoids, may influence immune cell recruitment, cytokine expression, and epithelial repair processes. Therefore, exploring the metabolic landscape in tandem with the microbiome may reveal functionally relevant pathways that contribute to the persistence and phenotype-specific progression of CRSwNP.
In this study, we applied an integrated omics approach combining 16S rRNA gene sequencing and untargeted metabolomics to characterize the sinonasal microbiome and tissue metabolome of patients with Eos- and nonEos-CRSwNP, alongside healthy controls. Our goal was to define phenotype-specific microbial and metabolic signatures, uncover functional microbial–metabolite interaction networks, and provide mechanistic insights that may inform biomarker development and personalized therapeutic strategies for CRSwNP.

## Materials and methods

### Study population and phenotype classification

Patients diagnosed with chronic rhinosinusitis with nasal polyps (CRSwNP) were prospectively enrolled and classified into eosinophilic (Eos-CRSwNP) and non-eosinophilic (nonEos-CRSwNP) subtypes based on histopathological evaluation of nasal polyp tissue. Hematoxylin and eosin (H&E) staining was performed, and two independent pathologists quantified the number of eosinophils per high-power field (HPF) [25]. A count of ≥10 eosinophils/HPF was defined as eosinophilic CRSwNP. Patients were eligible for inclusion if they were adults (≥18 years) diagnosed with chronic rhinosinusitis with nasal polyps (CRSwNP) according to EPOS 2020 criteria and scheduled to undergo endoscopic sinus surgery (ESS), during which both nasal polyp tissue and middle meatus swab samples could be obtained. Exclusion criteria included recent use (within 4 weeks) of systemic or topical corticosteroids, antibiotics, or nasal medications; presence of acute upper respiratory infection at the time of sampling; a history of malignancy, autoimmune disease, or immunodeficiency; prior treatment with biologic agents such as anti-IL-5, anti-IgE, or anti-IL-4Rα; and incomplete clinical or histopathological data. Age- and sex-matched healthy individuals undergoing septoplasty or concha bullosa correction served as controls. All participants provided written informed consent, and the study was approved by the institutional ethics committee of The Second Hospital of Shandong University (KYLL-2021(KJ)P-0241).

### Sample collection

For 16S rRNA gene sequencing, middle meatus swabs were collected intraoperatively from all CRSwNP patients and control individuals using sterile nylon swabs. Samples were immediately frozen in liquid nitrogen and stored at –80°C until DNA extraction. Nasal polyp tissue was obtained from CRSwNP patients during endoscopic sinus surgery procedures, and inferior

Table 1. The clinical characteristics at baseline of CRSwNP and control subjects.

| | Control | Non-EOS-CRSwNP | EOS-CRSwNP | P-value |
|---|---|---|---|---|
| Patients number n (%) | 14 (40%) | 7 (20%) | 14 (40%) | N/A |
| Age (years), mean±SD | 34.79 ± 15.13 | 43.71 ± 15.68 | 44.57 ± 10.10 | 0.13 |
| BMI (mean±SD) | 23.11 ± 2.167 | 23.63 ± 2.498 | 23.78 ± 2.430 | 0.78 |
| Sex, male, n (%) | 11 (78.57%) | 2 (28.57%) | 12 (85.71%) | 0.02 |
| Atopy, n (%) | 0 (0%) | 1 (14.29%) | 5 (35.71%) | 0.04 |
| History of smoking n (%) | 1 (7.14%) | 0 (0%) | 7 (50%) | 0.0024 |
| History of asthma n (%) | 1 (7.14%) | 0 (0%) | 2 (14.29%) | 0.53 |
| History of surgery n (%) | 0 (0%) | 1 (14.29%) | 1 (7.14%) | 0.40 |
| Eosinophils in blood (count, $*10^9$) | 0.1421 ± 0.09839 | 0.1857 ± 0.1861 | 0.6964 ± 0.7308 | 0.0001 |
| Eosinophils in tissue (count, n) | 1.214 ± 1.051 | 3.571 ± 2.507 | 69.29 ± 40.90 | <0.0001 |
| The Lund-Mackay CT score | 0.7143 ± 0.9139 | 11.86 ± 6.962 | 12.57± 3.975 | <0.0001 |

*Abbreviation. CRSwNP, chronic rhinosinusitis with nasal polyps. N/A, not applicable. $P < 0.05$ were considered significant.

turbinate tissue was collected from controls. All tissue samples were snap-frozen in liquid nitrogen and stored at –80°C prior to metabolomic analysis.

### Microbiome analysis via 16S rRNA sequencing

Microbial DNA was extracted using a commercial kit (MagPure DNA LQ kit, Magen Biotechnology Co., Ltd.) following manufacturer protocols. Negative controls (blank extraction controls and air-exposed swabs) were processed in parallel during DNA extraction and sequencing. No substantial amplification was observed in these controls. The V3–V4 hypervariable regions of the bacterial 16S rRNA gene were amplified using barcoded universal primers and sequenced on an Illumina MiSeq platform. Raw reads were quality-filtered, merged, and clustered into amplicon sequence variants (ASVs) using QIIME2 (v2022.2). Taxonomic assignment was performed against the SILVA 138 reference database. Alpha diversity (ACE, Chao1, Shannon, Simpson indices) and beta diversity (Bray–Curtis dissimilarity) were calculated. Non-metric multidimensional scaling (NMDS) was used for visualization. Differentially abundant taxa were identified using LEfSe with linear discriminant analysis (LDA) score threshold >2.0. Raw sequencing data were processed to obtain high-quality clean reads using a multi-step filtering approach. First, a 25 bp sliding window was applied to trim low-quality regions: if the average quality score within a window fell below Q20, reads were truncated, and sequences shorter than 75% of the original length were discarded. Reads with adapter contamination (defined as ≥15 bp overlap with ≤3 mismatches) were removed, as were those containing ambiguous bases (N) or exhibiting low complexity (≥10 consecutive identical bases). Demultiplexing was performed using exact barcode matching (0 mismatches), and primer sequences were verified to ensure accurate sample assignment. These steps were implemented to ensure the reliability and reproducibility of downstream microbial community analysiRaw sequencing data were processed to obtain high-quality clean reads using a multi-step filtering approach. First, a 25 bp sliding window was applied to trim low-quality regions: if the average quality score within a window fell below Q20, reads were truncated, and sequences shorter than 75% of the original length were discarded. Reads with adapter contamination (defined as ≥15 bp overlap with ≤3 mismatches) were removed, as were those containing ambiguous bases (N) or exhibiting low complexity (≥10 consecutive identical bases). Demultiplexing was performed using exact barcode matching (0 mismatches), and primer sequences were verified to ensure accurate sample assignment [26].

### Untargeted metabolomics analysis

Tissue samples were homogenized and extracted in methanol. After centrifugation and drying, metabolites were reconstituted and analyzed using ultra-high-performance liquid chromatography coupled with quadrupole time-of-flight mass spectrometry (UHPLC-QTOF-MS) in both positive and negative ion modes. Data were processed using XCMS for peak alignment, retention time correction, and normalization. Metabolites were annotated against public databases (HMDB, KEGG) and confirmed with authentic standards where available. Multivariate analysis, including principal component analysis (PCA) and orthogonal partial least squares discriminant analysis (OPLS-DA) was performed. Variable importance in projection (VIP) >1.0, $p < 0.05$, and fold change >2 were used to identify differentially expressed metabolites.

### Integration of microbiome and metabolomics data

Spearman correlation analysis was conducted to evaluate associations between the top 20 differentially abundant metabo-

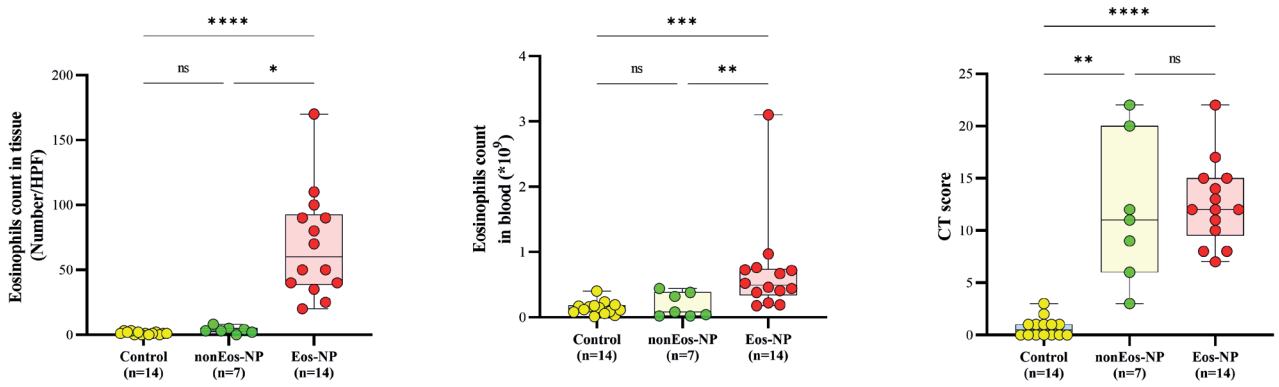


Figure 1. Clinical indicators of eosinophilic and non-eosinophilic CRSwNP compared to controls. (A) Eosinophil count in tissue (number per HPF) across control (n=14), non-eosinophilic CRSwNP (nonEos-NP, n=7), and eosinophilic CRSwNP (Eos-NP, n=14) groups. Eos-NP patients exhibited significantly higher tissue eosinophil infiltration compared to the other groups (****$p < 0.0001$, *$p < 0.05$). (B) Peripheral blood eosinophil count ($\times 10^9$/L) showing elevated levels in the Eos-NP group compared to both nonEos-NP and control groups (**$p < 0.01$, ***$p < 0.001$). No significant difference was found between the control and nonEos-NP. (C) Lund-Mackay CT scores assessing sinonasal disease severity. Both CRSwNP groups demonstrated significantly higher CT scores than controls (**$p < 0.01$, ****$p < 0.0001$), with no significant difference between Eos-NP and nonEos-NP groups.

lites and the top 20 bacterial genera. Correlation matrices were visualized as heat maps. Microbial-metabolite-pathway interaction networks were constructed using Cytoscape (v3.9.1), and enriched KEGG pathways were mapped to illustrate phenotype-specific biological functions.

### Statistical analysis

All statistical analyses were conducted using R (v4.2.1) and Python (v3.9). Kruskal-Wallis or Mann-Whitney U tests were used for intergroup comparisons. P-values were adjusted for multiple comparisons using the Benjamini-Hochberg false discovery rate (FDR) method. A two-sided $p < 0.05$ was considered statistically significant.

## Results

### Study subjects and phenotype classification

A total of 35 subjects were enrolled from January 2022 to March 2022 in the Department of Otolaryngology, The Second Hospital of Shandong University, including 14 eosinophilic CRSwNP (Eos-CRSwNP), 7 non-eosinophilic CRSwNP (nonEos-CRSwNP), and 14 healthy controls. The Eos-CRSwNP group exhibited significantly higher eosinophil counts in both peripheral blood and tissue compared to nonEos-CRSwNP and control groups (Figure 1A–B). The Lund-Mackay CT scores were also significantly elevated in both CRSwNP subgroups relative to controls (Figure 1C), confirming radiological severity. These findings validated the inflammatory and clinical distinction between the two CRSwNP phenotypes.

### Microbial community composition and diversity

16S rRNA sequencing revealed distinct microbial profiles among the three groups. Stacked bar plots showed genus-level distributions, with *Corynebacterium* and *Staphylococcus* dominating the control group, while Eos-CRSwNP samples were enriched in *Moraxella*, *Staphylococcus*, *Bacteroides*, and *Propionibacterium* (Figure 2A). In contrast, the nonEos-CRSwNP group had higher relative abundance of *Streptococcus*, *Anaerococcus*, and *Haemophilus*, suggesting phenotype-specific microbial shifts. Alpha diversity analysis demonstrated reduced microbial richness in Eos-CRSwNP (ACE and Chao1 indices) and reduced evenness (Shannon and Simpson indices) compared to controls (Figure 2B–E). The nonEos-CRSwNP group maintained intermediate diversity between Eos-CRSwNP and controls. NMDS plots based on Bray–Curtis dissimilarity revealed clear clustering between the three groups, with greater dispersion in Eos-CRSwNP, indicating higher inter-individual variability (Figure 2F).

LEfSe analysis identified multiple discriminative taxa. The control group was enriched in *Corynebacterium*, *Moraxella*, and *Lactobacillus*, while *Haemophilus* and *Bosea* were significantly enriched in nonEos-CRSwNP (Figure 2G). The Eos-CRSwNP group showed specific enrichment in members of *Enterobacteriaceae* and *Bradyrhizobiaceae*, suggesting potential roles in eosinophilic inflammation. Additionally, *Brevibacillus* abundance was significantly lower in Eos-CRSwNP compared to nonEos-CRSwNP (Figure 2H).

### Metabolomic profiles in CRSwNP phenotypes

PCA and OPLS-DA plots confirmed the metabolic separation between CRSwNP phenotypes and controls (Figure 3A–C). Distinct clusters were observed for Eos-CRSwNP vs. control and nonEos-CRSwNP vs. control. Volcano plots identified significantly altered metabolites (VIP >1, $p < 0.05$, FC > 2). Eos-CRSwNP exhibited elevated levels of fumaric acid, linoleic acid, and arachidonic acid (Figure 3D), reflecting alterations in oxidative

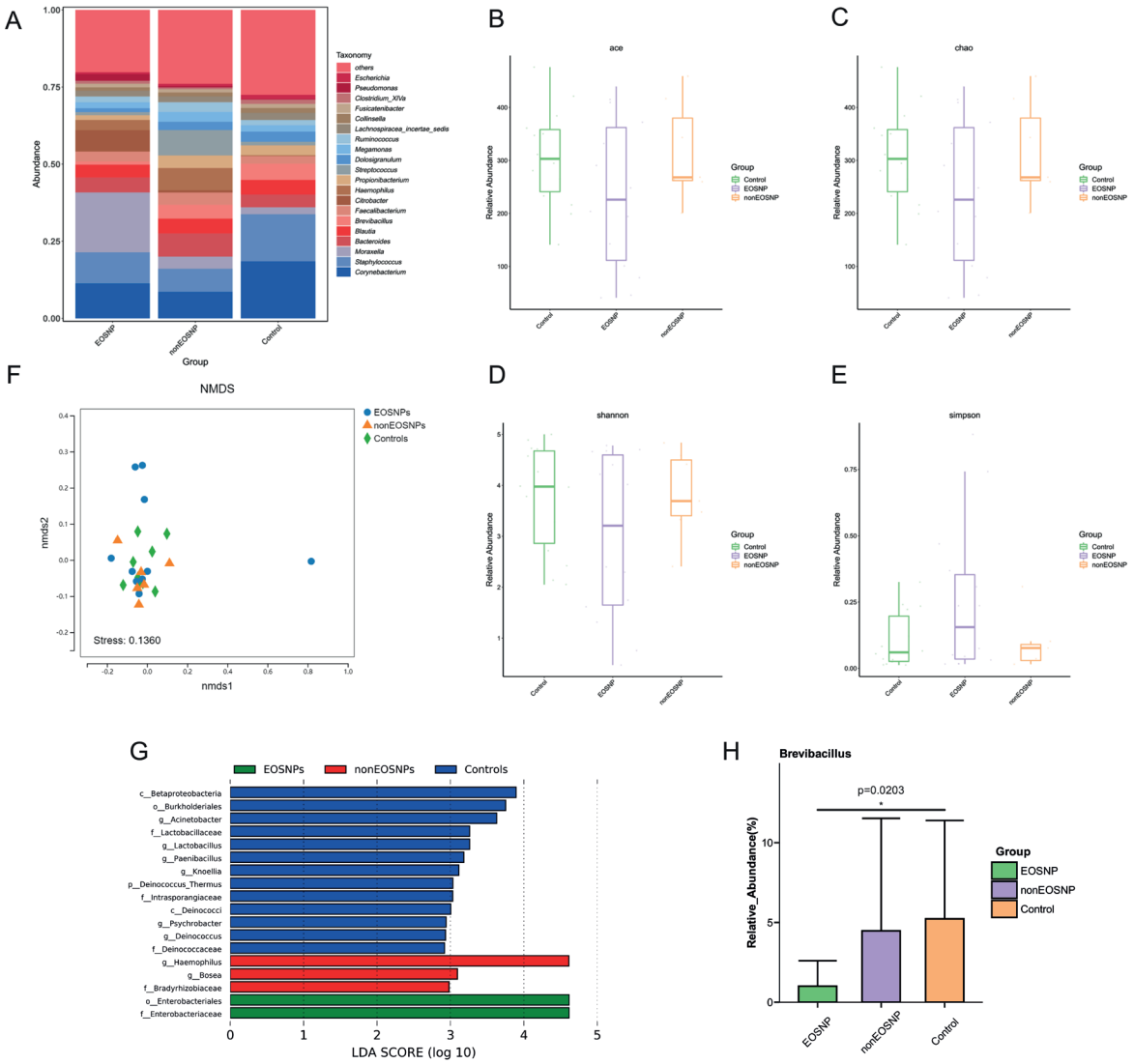


Figure 2. Microbial community composition, diversity, and key taxa differences in EOS-CRSwNP, nonEOS-CRSwNP, and control groups. (A) Stacked bar plot showing the relative abundance of bacterial genera across the three groups [(EOS-CRSwNP, n=14), (nonEOS-CRSwNP, n=7) and (Controls, n=14)]. Each color represents a different genus. Distinct microbial compositions are evident between phenotypes. (B) Alpha diversity (ACE index) illustrates species richness across groups. Lower ACE scores were observed in the CRSwNP groups (n=21) compared to controls (n=14). (C) Alpha diversity (Chao1 index) evaluating species richness. Results show altered richness patterns in disease phenotypes. (D) Alpha diversity (Shannon index) reflects both the richness and evenness of bacterial communities. EOS-CRSwNP (n=14) shows a trend toward reduced diversity. (E) Alpha diversity (Simpson index) assessing community evenness. The EOS-CRSwNP group (n=14) presents lower evenness compared to other groups. (F) Non-metric multidimensional scaling (NMDS) plot based on Bray-Curtis distance showing beta diversity differences. Clear clustering indicates distinct microbial community structures among the three groups (stress value = 0.1360). (G) LEfSe analysis shows bacterial taxa significantly enriched in each group, based on LDA score (log10 > 2.0). Blue bars: taxa enriched in controls; red: enriched in nonEOS-CRSwNP (n=7); green: enriched in EOS-CRSwNP(n=14). (H) Box plot of relative abundance of *Brevibacillus* across groups. A significantly higher abundance was observed in the nonEOS-CRSwNP group (n=7) compared to EOS-CRSwNP (n=14) (p = 0.0203).

phosphorylation and lipid metabolism. In contrast, nonEos-CRSwNP was enriched in L-glutamine, taurine, and ethanolamine phosphate (Figure 3E), implicating shifts in nitrogen and amino acid metabolism. KEGG pathway enrichment revealed that core DEMs in Eos-CRSwNP were associated with the tricarboxylic acid (TCA) cycle, linoleic acid metabolism, and oxidative phosphorylation (Figure 3G). For nonEos-CRSwNP, enriched pathways included amino acid biosynthesis, taurine metabolism, and phospholipid metabolism (Figure 3I). Corresponding heatmaps showed a clear separation of metabolite patterns among phenotypes (Figure 3F, 3H).

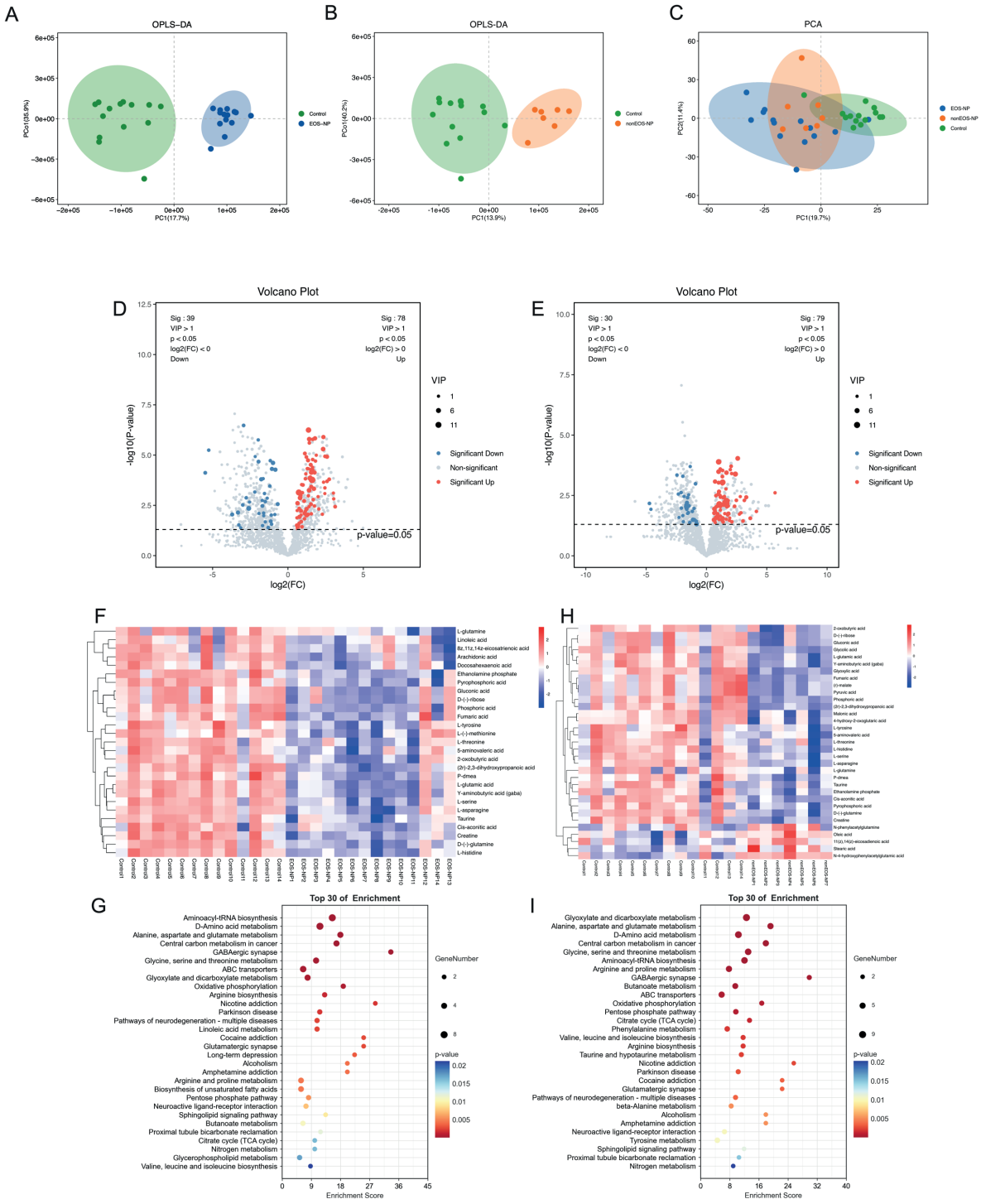


Figure 3. Identification and functional enrichment of core differential metabolites (Core DEMs) between CRSwNP phenotypes. (A) OPLS-DA score plot [EOS-NP (n=14) vs Control (n=14))] showing distinct clustering between eosinophilic CRSwNP (EOS-NP, n=14) and healthy controls based on metabolomic profiles. (B) OPLS-DA score plot (nonEOS-NP, n=7 vs Control, n=14) showing clear metabolic separation between non-eosinophilic CRSwNP (nonEOS-NP, n=7) and controls. (C) Principal Component Analysis (PCA) plot illustrating the overall distribution of all three groups [(EOS-CRSwNP, n=14), (nonEOS-CRSwNP, n=7) and (Controls,n=14)] in the metabolomic space. (D) Volcano plot (EOS-NP, n=14 vs Control, n=14) displaying significantly upregulated (red) and downregulated (blue) metabolites. Core DEMs are defined as those significantly altered and enriched in functional pathways. (E) Volcano plot (nonEOS-NP, n=7 vs Control, n=14) showing metabolite distribution with similar annotation. Significance thresholds: $|\log_2 FC| > 1$, $p < 0.05$, VIP > 1. (F) Heatmap of differential metabolites (EOS-NP, n=14 vs Control, n=14) showing relative abundance across samples, clustered by both metabolite and sample similarity. (G) Top 30 enriched pathways (EOS-NP, n=14 vs Control, n=14) based on KEGG analysis. Core DEMs contribute significantly to pathways such as amino acid metabolism and TCA cycle. (H) Heatmap of differential metabolites (nonEOS-NP, n=7 vs Control, n=14) highlighting distinct metabolic signatures compared to EOS-NP(n=14). (I) Top 30 enriched pathways (nonEOS-NP, n=7 vs Control, n=14) revealing significant enrichment in pathways including glycerolipid metabolism, taurine and hypotaurine metabolism, and purine metabolism.

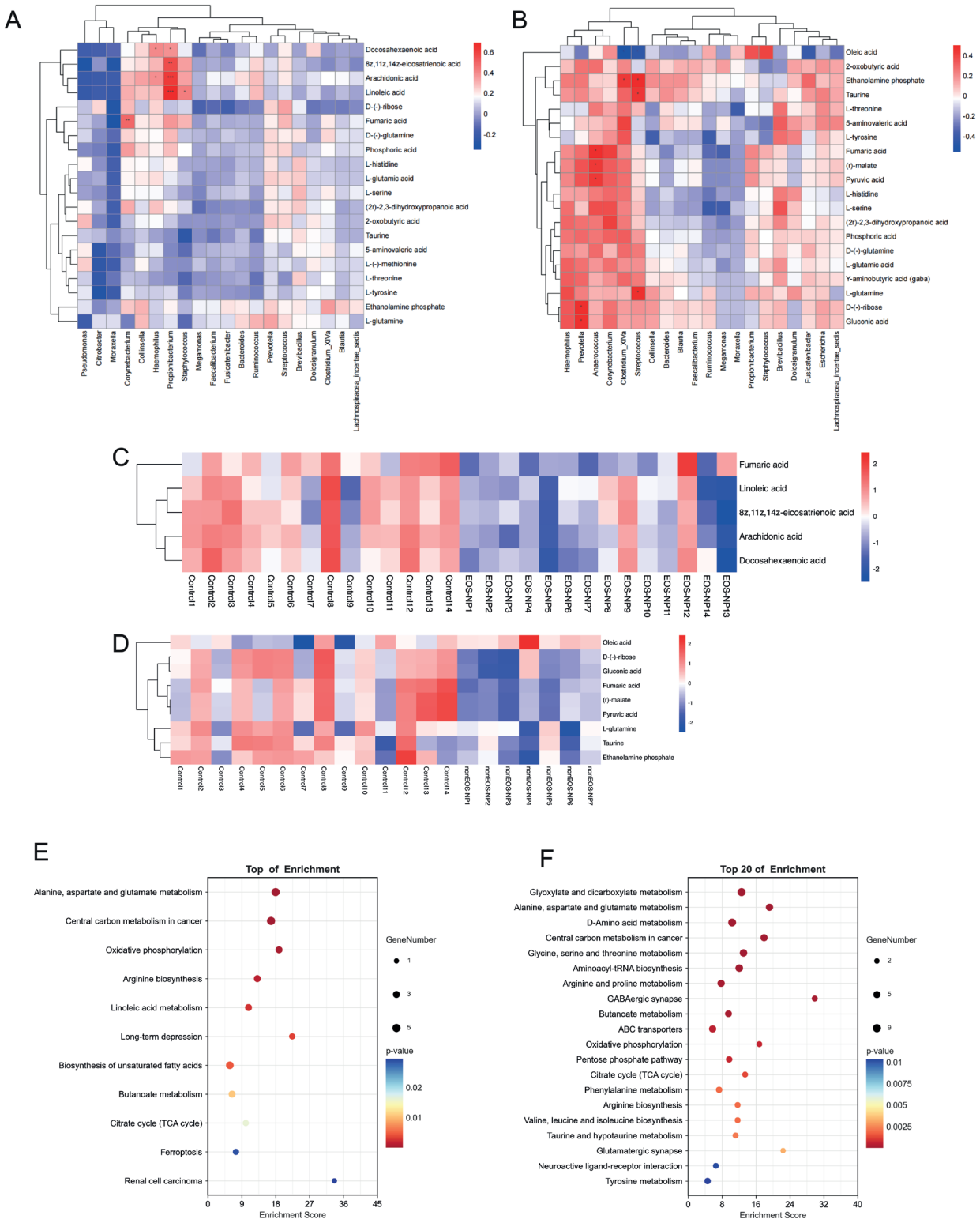


Figure 4. Correlation analysis between core differential metabolites and dominant bacterial genera in CRSwNP subtypes. (A) Heatmap of metabolite–bacteria correlations in EOS-CRSwNP group(n=14). Spearman correlation coefficients between the top 20 core differential metabolites and the top 20 high-abundance bacterial genera are shown. Red indicates a positive correlation; blue indicates a negative correlation. (B) Heatmap of metabolite–bacteria correlations in the nonEOS-CRSwNP group(n=7). The correlation pattern differs from EOS-CRSwNP(n=7), highlighting phenotype-specific microbiota–metabolite interactions. (C) Zoomed-in heatmap showing selected metabolite–bacteria associations in the EOS-CRSwNP group (n=14)with strong correlations. (D) Zoomed-in heatmap of representative core associations in the nonEOS-CRSwNP group(n=7). (E) Enrichment analysis of pathways associated with bacteria-correlated core metabolites in the EOS-CRSwNP group(n=14). The dot plot shows enriched KEGG pathways, with dot size representing the number of mapped genes and color indicating p-values. (F) Enrichment analysis of pathways for the nonEOS-CRSwNP group (n=7) based on correlated core metabolites. Pathways related to energy metabolism, amino acid biosynthesis, and neuroactive signaling are prominent.

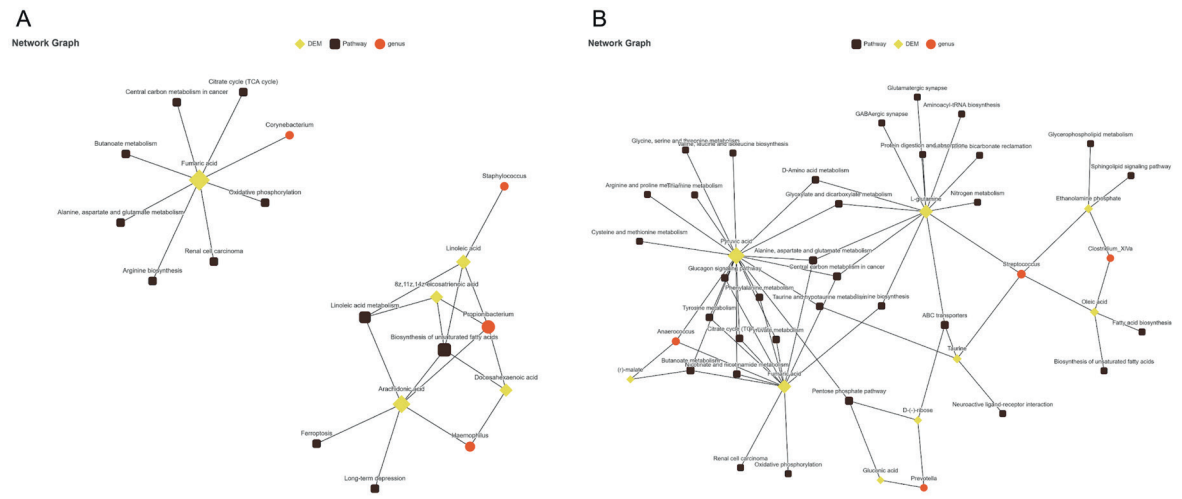


Figure 5. Integrated network of core differential metabolites, key bacterial genera, and enriched pathways in CRSwNP subtypes. (A) Network graph of the EOS-CRSwNP group. The figure visualizes the interactions among core differential metabolites (yellow diamonds), significantly enriched KEGG pathways (brown squares), and top correlated bacterial genera (red circles) specific to the eosinophilic CRSwNP phenotype. The graph reveals a relatively compact network with focused associations between metabolites such as fumaric acid and genera including Fusobacterium and Streptococcus, and their linked metabolic pathways (e.g., TCA cycle, butanoate metabolism). (B) Network graph of the nonEOS-CRSwNP group. A more complex and expanded interaction network is shown, indicating broader connectivity between core metabolites, dominant genera, and a larger variety of enriched pathways. Notable metabolites like glucuronic acid and L-glutamic acid are central to multiple modules, linking to bacteria such as *Lactobacillus* and *Clostridium* sensu stricto 1, and pathways related to amino acid metabolism, ABC transporters, and bile acid biosynthesis.

### Microbiota–metabolite correlation networks

Spearman correlation analysis between the top 20 core metabolites and top 20 bacterial genera revealed phenotype-specific interaction matrices (Figure 4A–B). In Eos-CRSwNP, positive correlations were observed between *Staphylococcus* and linoleic acid, and *Corynebacterium* with fumaric acid. *Haemophilus* and *Propionibacterium* showed links to arachidonic acid (Figure 4C). In nonEos-CRSwNP, *Streptococcus* and *Clostridium XlVa* were correlated with L-glutamine and taurine, while *Anaerococcus* and *Prevotella* were associated with pyruvate and D-ribose (Figure 4D). *Bacteroides* showed strong correlations with ethanolamine phosphate. Pathways associated with microbiota-correlated metabolites included linoleic acid metabolism, oxidative phosphorylation, and arachidonic acid metabolism in Eos-CRSwNP (Figure 4E). NonEos-CRSwNP correlated pathways involved amino acid metabolism, ABC transporters, and glutamatergic signaling (Figure 4F), highlighting distinct biochemical landscapes.

### Integrated metabolic–microbial–pathway networks

Integrated multi-omic networks were constructed to visualize phenotype-specific interactions (Figure 5). In Eos-CRSwNP, the network was dominated by lipid metabolism nodes such as fumaric acid and linoleic acid, with hub genera including *Staphylococcus* and *Corynebacterium* (Figure 5A). In nonEos-CRSwNP, the network was more complex, centered around nitrogen and amino acid metabolism, with key interactions involving *Streptococcus*, *Clostridium sensu stricto 1*, and metabolites such as L-glutamine and taurine (Figure 5B). These interaction modules suggest distinct inflammatory microenvironments and microbial–metabolite crosstalk between CRSwNP phenotypes.

## Discussion

In this study, we applied an integrative multi-omics approach to dissect the microbial and metabolic signatures underlying eosinophilic (Eos-CRSwNP) and non-eosinophilic (nonEos-CRSwNP) subtypes of chronic rhinosinusitis with nasal polyps. By combining 16S rRNA-based microbiome profiling and untargeted metabolomics, we uncovered phenotype-specific microbial-metabolite interaction networks, which may underlie the immunological and clinical heterogeneity observed between the two disease subtypes.

Our results demonstrated that Eos-CRSwNP was characterized by reduced microbial richness and evenness, with a relative overgrowth of *Staphylococcus aureus* and *Corynebacterium* as determined by α-diversity indices (ACE, Chao1, Shannon, Simpson) and β-diversity. These findings are consistent with previous studies linking *S. aureus* colonization and enterotoxin production to Type 2 inflammation in CRSwNP, promoting eosinophilic infiltration and IgE elevation [27, 28]. Conversely, nonEos-CRSwNP exhibited higher microbial diversity and enrichment of facultative anaerobes such as *Streptococcus*, *Anaerococcus*, and *Clostridium XlVa*, genera more commonly associated with neutrophilic or mixed inflammation and Th1/Th17-skewed responses [29-32]. Also, in this study, *Brevibacillus* was the only genus showing a statistically significant difference among the three groups, with

a notably lower abundance in the Eos-CRSwNP group. Although its biological role in CRSwNP remains unclear, the reduced abundance of *Brevibacillus* in Eos-CRSwNP may reflect the loss of microbial diversity and potentially protective commensals in the context of eosinophilic inflammation, rather than a direct pathogenic effect. This observation warrants further investigation into its possible interaction with type 2–dominant inflammatory responses. These distinct microbial patterns suggest that dysbiosis in Eos-CRSwNP may involve a loss of microbial balance, favoring the proliferation of pro-inflammatory pathobionts. In contrast, the broader diversity in nonEos-CRSwNP may reflect a less severe but more complex dysbiotic environment, potentially driven by environmental exposure or epithelial barrier dysfunction.

Untargeted metabolomics revealed clear differences in metabolic pathways between CRSwNP phenotypes. Eos-CRSwNP showed elevated fumaric acid, linoleic acid, and arachidonic acid—metabolites implicated in oxidative stress and eicosanoid-driven inflammation [33-35]. Notably, the upregulation of arachidonic acid metabolism aligns with known mechanisms of eosinophilic inflammation, as its downstream products like leukotrienes promote eosinophil chemotaxis and degranulation [36]. In contrast, nonEos-CRSwNP displayed increased levels of L-glutamine, taurine, and ethanolamine phosphate. These metabolites suggest the involvement of amino acid metabolism and phospholipid turnover. Glutamine, an essential fuel for activated immune cells, may support neutrophilic responses, while taurine could reflect compensatory antioxidant activity or altered bile acid biosynthesis [37,38]. Phospholipid intermediates like ethanolamine phosphate may also impact membrane remodeling and cell signaling [39]. These distinct metabolic fingerprints highlight the divergent immunometabolic reprogramming between Eos- and nonEos-CRSwNP, suggesting that metabolite signaling plays an active role in shaping local inflammation.

By integrating microbial and metabolic data, we observed tightly linked microbial-metabolite modules in each CRSwNP subtype. In Eos-CRSwNP, *Staphylococcus* correlated positively with linoleic acid metabolism and *Corynebacterium* with fumaric acid, suggesting a possible microbial contribution to lipid-driven inflammation and mitochondrial dysfunction. *Haemophilus* and *Propionibacterium* were also linked to arachidonic acid metabolism, further implicating microbial modulation of eicosanoid biosynthesis. In nonEos-CRSwNP, *Streptococcus* and *Clostridium XlVa* were associated with L-glutamine and taurine metabolism, pathways often tied to nitrogen balance and immune cell energetics. The identification of *Bacteroides* linked to ethanolamine phosphate suggests potential microbial influence on phospholipid remodeling. These findings underscore the importance of microbial-derived metabolites as potential mediators of local immune activation and phenotype-specific inflammation in CRSwNP. Consistent with this, recent evidence has shown that specific microbial-derived metabolites such as butyrate can suppress type 2 inflammation in eosinophilic CRSwNP by modulating epithelial and immune responses, further supporting their potential as therapeutic targets [40].

The consistent enrichment of *Staphylococcus aureus* and elevated linoleic/arachidonic acid levels in Eos-CRSwNP suggest a potential inflammatory axis that may be targetable through microbiome modulation or lipid mediator blockade. These components may reflect distinct features for endotype differentiation or disease monitoring, pending further validation. Conversely, metabolites such as glutamine and taurine, enriched in nonEos-CRSwNP, may reflect distinct immune-metabolic regulation and could guide personalized anti-inflammatory strategies. The identification of phenotype-specific microbial and metabolic signatures suggests that CRSwNP patients may benefit from precision medicine approaches. For Eos-CRSwNP, strategies targeting *S. aureus* colonization, arachidonic acid metabolism, or mitochondrial ROS production could modulate inflammation. For nonEos-CRSwNP, interventions aiming to restore microbial diversity or normalize amino acid metabolism may be beneficial. Moreover, selected core differential metabolites (e.g., fumaric acid, glutamine) and genera (e.g., *Staphylococcus*, *Streptococcus*) may serve as potential biomarkers for disease classification and monitoring. This study has several limitations that should be acknowledged. First, the cross-sectional design precludes causal inference, limiting our ability to determine whether the observed microbial and metabolic changes are drivers or consequences of CRSwNP pathogenesis. Longitudinal or interventional studies are warranted to explore causal relationships and temporal dynamics. Second, the relatively small sample size, particularly in the non-eosinophilic CRSwNP group, limited our ability to perform robust subgroup or multivariate analyses that controlled for confounding variables such as age, sex, smoking, atopy, asthma, and BMI. Third, while efforts were made to minimize external contamination—including the use of negative controls and decontamination steps—low-biomass samples such as nasal swabs inherently carry a risk of environmental microbial interference. Fourth, although samples were collected over a narrow time window to reduce variability, seasonal influences on the microbiome and metabolome were not systematically addressed, and time-series sampling would be valuable in future studies. Fifth, the microbiome and metabolome were assessed from different sample types (swabs vs. tissues), which may complicate direct comparisons. Sixth, our classification relied solely on eosinophil counts, which may not fully capture the immunologic spectrum of CRSwNP endotypes. Additionally, the use of "untargeted metabolomics" did not encompass the entire metabolome, and future studies should

aim to extend coverage and include functional validation of key microbial metabolite pathways. Finally, while the study identifies potential microbial and metabolic signatures with diagnostic or therapeutic promise, we did not evaluate their clinical utility (e.g., sensitivity, specificity, AUC) and therefore refer to them only as preliminary candidates for future biomarker validation. Future studies should expand sample size, include longitudinal follow-up, and incorporate additional omics layers such as transcriptomics or proteomics. Functional validation of key microbial-metabolite interactions using in vitro or in vivo models will be essential to establish causality and therapeutic relevance.
In summary, our integrative omics analysis delineaed distinct microbial-metabolite crosstalk in eosinophilic and non-eosinophilic CRSwNP. These findings provide mechanistic insights into disease heterogeneity and may contribute to the identification of endotype-associated patterns that support phenotype-guided research and individualized therapeutic approaches, rather than serving as validated clinical biomarkers.

## Conclusion

In this study, we performed an integrated analysis of the sinonasal microbiome and metabolome in patients with eosinophilic and non-eosinophilic chronic rhinosinusitis with nasal polyps (CRSwNP), revealing distinct microbial compositions, metabolic profiles, and interaction networks between the two phenotypes. Eosinophilic CRSwNP showed reduced microbial diversity and was associated with lipid- and energy-related metabolic alterations, while non-eosinophilic CRSwNP displayed greater microbial richness and distinct shifts in amino acid and nitrogen metabolism. Through correlation analysis and network mapping, we identified phenotype-specific links between key bacterial genera and differential metabolites, suggesting that microbial activity may shape the local inflammatory environment in a subtype-dependent manner. These findings offer new insights into the underlying mechanisms of CRSwNP and provide a potential foundation for the development of more personalized diagnostic and therapeutic approaches.

## Author contributions

HZ, XZ, XL, LZ, PJ conceptualized and designed the study, contributed to data analysis, and participated in manuscript preparation. XZ, XL, PJ performed microbiome analysis and statistical analysis. XL, LZ provided valuable insights into study design and manuscript revision. TG and HZ assisted in tissue sample collection and preparation. HZ and XL contributed to metabolomics data analysis and figure preparation. HZ, XZ, XL, LZ, PJ were involved in patient recruitment and specimen collection, managed clinical metadata, interpreted microbiome and metabolomics data, and played major roles in writing and critically reviewing the manuscript. All authors read and approved the final manuscript.

## Acknowledgments

None

## Ethics approval and consent to participate

This study was approved by the institutional review board.

## Conflict of interest

The authors declare that they have competing interests.

## Funding

This research was supported by the National Natural Science Foundation of China (81800885, 82101195) and the Shandong Provincial Natural Science Foundation (ZR2022MH283, ZR2024QH195).

## Data availability

All data included in this study are available upon request by contact with the corresponding author.

## References

1. Kwah JH, Peters AT. Nasal polyps and rhinosinusitis. Allergy Asthma Proc. 2019;40(6):380-4.
2. Bandi S, Stephen E, Bansal K, Mahdavinia M. Understanding the CRSwNP patient as whole. Am J Rhinol Allergy. 2023;37(2):140-6.
3. Cho SH, Hamilos DL, Han DH, Laidlaw TM. Phenotypes of chronic rhinosinusitis. J Allergy Clin Immunol Pract. 2020;8(5):1505-11.
4. Bayar Muluk N, Cingi C, Scadding GK, Scadding G. Chronic rhinosinusitis-could phenotyping or endotyping aid therapy? Am J Rhinol Allergy. 2019;33(1):83-93.
5. Xie X, Xuan L, Zhao Y, Wang X, Zhang L. Diverse endotypes of chronic rhinosinusitis and clinical implications. Clin Rev Allergy Immunol. 2023;65(3):420-32.
6. Kato A, Peters AT, Stevens WW, Schleimer RP, Tan BK, Kern RC. Endotypes of chronic rhinosinusitis: relationships to disease phenotypes, pathogenesis, clinical findings, and treatment approaches. Allergy. 2022;77(3):812-26.
7. Bachert C, Hicks A, Gane S, et al. The interleukin-4/interleukin-13 pathway in type 2 inflammation in chronic rhinosinusitis with nasal polyps. Front Immunol. 2024;15:1356298.
8. Kariyawasam HH. Chronic rhinosinusitis with nasal polyps: mechanistic insights from targeting IL-4 and IL-13 via IL-4Rα inhibition with dupilumab. Expert Rev Clin Immunol. 2020;16(12):1115-25.
9. Ho J, Hamizan AW, Alvarado R, Rimmer J, Sewell WA, Harvey RJ. Systemic predictors of eosinophilic chronic rhinosinusitis. Am J Rhinol Allergy. 2018;32(4):252-7.
10. Nazari J, Shahba F, Jafariaghdam N, et al. Immune endotyping and gene expression profile of patients with chronic rhinosinusitis with nasal polyps in the aspirin-exacerbated respiratory disease (AERD) and the non-AERD subgroups. Allergy Asthma Clin Immunol. 2024;20(1):14.
11. Fokkens WJ, Viskens AS, Backer V, et al. EPOS/EUFOREA update on indication and evaluation of biologics in chronic rhinosinusitis with nasal polyps 2023. Rhinology. 2023;61(3):194-202.
12. Bachert C, Zhang N, Cavaliere C, Weiping W, Gevaert E, Krysko O. Biologics for chronic rhinosinusitis with nasal polyps. J Allergy Clin Immunol. 2020;145(3):725-39.
13. Ruan JW, Zhao JF, Li XL, et al. Characterizing the neutrophilic inflammation in chronic rhinosinusitis with nasal polyps. Front Cell Dev Biol. 2021;9:793073.
14. Wang W, Gao Y, Zhu Z, et al. Changes in the clinical and histological characteristics of Chinese

chronic rhinosinusitis with nasal polyps over 11 years. Int Forum Allergy Rhinol. 2019;9(2):149-57.
15. Liang Y, Xie R, Xiong X, et al. Alterations of nasal microbiome in eosinophilic chronic rhinosinusitis. J Allergy Clin Immunol. 2023;151(5):1286-95.e2.
16. Gan W, Zhang H, Yang F, Liu S, Liu F, Meng J. The influence of nasal bacterial microbiome diversity on the pathogenesis and prognosis of chronic rhinosinusitis patients with polyps. Eur Arch Otorhinolaryngol. 2021;278(4):1075-88.
17. Gan W, Zhang H, Yang F, Liu S, Liu F, Meng J. The influence of nasal microbiome diversity and inflammatory patterns on the prognosis of nasal polyps. Sci Rep. 2021;11(1):6364.
18. Gan W, Xiang Y, Wei B, Liu S, Liu F. The inflammatory microenvironment of nasal polyps in patients with chronic rhinosinusitis and the relationship of this microenvironment with the nasal microbiome. Asian J Surg. 2024;47(1):124-33.
19. Kaliniak S, Fiedoruk K, Spałek J, Piktel E, Durnaś B, Góźdź S, et al. Remodeling of paranasal sinuses mucosa functions in response to biofilm-induced inflammation. J Inflamm Res. 2024;17:1295-323.
20. Gómez-García M, Moreno-Jimenez E, Morgado N, et al. The role of the gut and airway microbiota in chronic rhinosinusitis with nasal polyps: a systematic review. Int J Mol Sci. 2024;25(15).
21. Gan W, Yang F, Tang Y, et al. The difference in nasal bacterial microbiome diversity between chronic rhinosinusitis patients with polyps and a control population. Int Forum Allergy Rhinol. 2019;9(6):582-92.
22. Xu Z, Huang Y, Meese T, et al. The multi-omics single-cell landscape of sinus mucosa in uncontrolled severe chronic rhinosinusitis with nasal polyps. Clin Immunol. 2023;256:109791.
23. Chen CL, Ma J, Lu RY, et al. Perturbated glucose metabolism augments epithelial cell proinflammatory function in chronic rhinosinusitis. J Allergy Clin Immunol. 2023;151(4):991-1004.e20.
24. Yang Y, Guo J, Yao Y, et al. Proteomics and metabolomics analysis of nasal lavage fluid in chronic rhinosinusitis with nasal polyps. Int Forum Allergy Rhinol. 2023;13(10):1966-70.
25. Fokkens WJ, Lund VJ, Hopkins C, Hellings PW, Kern R, Reitsma S, et al. European position paper on rhinosinusitis and nasal polyps 2020. Rhinology. 2020;58(Suppl S29):1-464.
26. Bolyen E, Rideout JR, Dillon MR, et al. Reproducible, interactive, scalable and extensible microbiome data science using QIIME 2. Nat Biotechnol. 2019;37(8):852-7.
27. Shaghayegh G, Cooksley C, Ramezanpour M, Wormald PJ, Psaltis AJ, Vreugde S. Chronic rhinosinusitis, S. aureus biofilm and secreted products, inflammatory responses, and disease severity. Biomedicines. 2022;10(6).
28. Calabrese C, Seccia V, Pelaia C, Spinelli F, Morini P, Rizzi A, Detoraki A. S. aureus and IgE-mediated diseases: pilot or copilot? A narrative review. Expert Rev Clin Immunol. 2022;18(6):639-47.
29. Chen J, Yang S, Li W, et al. IL-17A secreted by Th17 cells is essential for the host against Streptococcus agalactiae infections. J Microbiol Biotechnol. 2021;31(5):667-75.
30. Lundgren A, Bhuiyan TR, Novak D, et al. Characterization of Th17 responses to Streptococcus pneumoniae in humans: comparisons between adults and children in a developed and a developing country. Vaccine. 2012;30(26):3897-907.
31. Uzunoğlu E, Kalkancı A, Kılıç E, Kızıl Y, Aydil U, Diker KS, Uslu SS. Bacterial and fungal communities in chronic rhinosinusitis with nasal polyps. PLoS One. 2024;19(5):e0304634.
32. Wang F, Liu Q, Wu H, Tang T, Zhao T, Li Z. The dysbiosis gut microbiota induces the alternation of metabolism and imbalance of Th17/Treg in OSA patients. Arch Microbiol. 2022;204(4):217.
33. Khoury S, Gudziol V, Grégoire S, et al. Lipidomic profile of human nasal mucosa and associations with circulating fatty acids and olfactory deficiency. Sci Rep. 2021;11(1):16771.
34. Xie S, Zhang H, Liu Y, Gao K, Zhang J, Fan R, et al. The role of serum metabolomics in distinguishing chronic rhinosinusitis with nasal polyp phenotypes. Front Mol Biosci. 2020;7:593976.
35. Trostchansky A, Wood I, Rubbo H. Regulation of arachidonic acid oxidation and metabolism by lipid electrophiles. Prostaglandins Other Lipid Mediat. 2021;152:106482.
36. Xu X, Li J, Zhang Y, Zhang L. Arachidonic acid 15-lipoxygenase: effects of its expression, metabolites, and genetic and epigenetic variations on airway inflammation. Allergy Asthma Immunol Res. 2021;13(5):684-96.
37. Cruzat V, Macedo Rogero M, Noel Keane K, Curi R, Newsholme P. Glutamine: metabolism and immune function, supplementation and clinical translation. Nutrients. 2018;10(11).
38. Jong CJ, Sandal P, Schaffer SW. The role of taurine in mitochondria health: more than just an antioxidant. Molecules. 2021;26(16).
39. Calzada E, Onguka O, Claypool SM. Phosphatidylethanolamine metabolism in health and disease. Int Rev Cell Mol Biol. 2016;321:29-88.
40. Toyama M, Kouzaki H, Shimizu T, Hirakawa H, Suzuki M. Butyrate inhibits type 2 inflammation in eosinophilic chronic rhinosinusitis. Biochem Biophys Res Commun. 2024;714:149967.

Peng Jin
Department of Otolaryngology
The Second Qilu Hospital of Shandong University
247 Beiyuan Avenue
Jinan
Shandong 250033
China

E-mail: jinpeng0215@126.com

Lili Zhi
Department of Allergy
The First Affiliated Hospital of Shandong First Medical University
Shandong Provincial Qianfoshan Hospital
Shandong Institute of Respiratory Diseases
Jinan
Shandong 250014
China

E-mail:qfsyyallergy@163.com

Hailing Zhang[1,#], Xiaoxue Zi[1,#], Xu Li[2], Tingting Gao[2], Hongping Zhang[1], Hongyang Zhang[1], Xu Liang[1], Lili Zhi[2,*], Peng Jin[1,*]

[1] Department of Otolaryngology, The Second Qilu Hospital of Shandong University, Jinan, Shandong, China

[2] Department of Allergy, The First Affiliated Hospital of Shandong First Medical University, Shandong Provincial Qianfoshan Hospital, Shandong Institute of Respiratory Diseases, Jinan, China

#, * equal contribution

**Rhinology 64: 2,** 0 - 0, 2026
https://doi.org/10.4193/Rhin25.166

**Received for publication:**
March 27, 2025
**Accepted:** October 28, 2025

**Associate Editor:**
Sanna Toppila-Salmi